

Communication

Probing Synergies between Lignin-Rich and Cellulose Compounds for Gasification

Martin J. Taylor ^{1,2}, Apostolos K. Michopoulos ³, Anastasia A. Zabaniotou ⁴ and Vasiliki Skoulou ^{1,2,*}

¹ Energy and Environment Institute, University of Hull, Cottingham Road, Hull HU6 7RX, UK; Martin.Taylor@hull.ac.uk

² B3 Challenge Group, Department of Chemical Engineering, University of Hull, Cottingham Road, Hull HU6 7RX, UK

³ Energy and Environmental Design of Buildings Research Lab, University of Cyprus, P.O. Box 20537, Nicosia 1678, Cyprus; michopoulos.apostolos@ucy.ac.cy

⁴ Department of Chemical Engineering, Aristotle University of Thessaloniki, P.O. Box 455, GR 541 24 Thessaloniki, Greece; azampani@auth.gr

* Correspondence: v.skoulou@hull.ac.uk

Received: 22 April 2020; Accepted: 17 May 2020; Published: 20 May 2020



Abstract: The fixed-bed gasification of lignin-rich and -deficient mixtures was carried out to probe the synergistic effects between two model compounds, Lignin Pink (LP) rich in Na and Cellulose Microcrystalline (CM). Reaction conditions utilized the most commonly used air ratios in current wood gasifiers at 750 and 850 °C. It was found that by increasing the lignin content in the mixture, there was a selectivity change from solid to gas products, contrary to a similar study previously carried out for pyrolysis. This change in product mix was promoted by the catalytic effect of Na edge recession deposits on the surface of the char. As a result, the water gas shift reaction was enhanced at 850 °C for the LP₄₈CM₅₂ mixture across all air ratios. This was evidenced by a strong correlation between the produced H₂ and CO_x. Meanwhile, by lowering the lignin content in the mixtures, the reactivity of cellulose microcrystalline was found to generate more char at higher temperatures, similar to lignin mixtures when undergoing pyrolysis.

Keywords: gasification; lignocellulosic biomass waste; lignin; cellulose; Na promotion; water gas shift

1. Introduction

The utilization of sustainable solid fuels such as woody wastes is one of many possible answers to combat irreversible climate change damage, attributed to the extensive usage of fossil-based fuels such as coal and the corresponding CO₂ emissions produced [1]. One method of replacing the polluting coal, rich in mineral ash constituents, is the use of biorenewable feedstocks, specifically lignocellulosic biomass wastes whereupon the carbon cycle can be closed. This can also be done by co-processing or blending the coal feed with other wastes such as pulps, pyrolysis tars or lignin-rich biorefinery sludges and even other biodegradable by-products. Here, the overall net CO₂ emissions can be reduced to zero as a part of the natural carbon cycle, or even to negative if used in conjunction with modern carbon capture technologies [2]. Currently, a popular feedstock used on a large scale for bioenergy production is woody biomass residues; these are physically, chemically or physicochemically pretreated [3,4] and fed into thermochemical reactors for pyrolysis (mainly solid to liquid thermal cracking reactions) [5–7], gasification or combustion (mainly solid to gas, gas to gas and thermochemical cracking reactions) [8,9]. However, variability of the lignocellulosic biomass waste is a limiting factor in the use of large-scale waste reformation for the production of low-carbon energy [10]. This is due to wide variations in

cellulose, hemicellulose and lignin ratios, depending on the feedstock (woody vs. herbaceous). As a result, the chemical interactions and bonding bring in a new paradigm as the feedstocks will each have differences in the required energy to thermally decompose. Additionally, the presence and role of any inorganic ash constituents that may be present in the substrate, such as Na, K, S, Ca, Si, Mg or Cl, must be considered. These elements form compounds that can cause extensive damage to reactor systems and promote side reactions that cause fouling, slagging and de-fluidization. Ultimately, this leads to a breakdown in combustible fuel gas production [11,12]. Additionally, inorganic components can catalyze the production of specific gas products or produce toxic emissions in their own right such as H₂S or HCl [13,14].

Work published by Volpe, Zabaniotou and Skoulou in 2018 found that there is a synergistic effect between lignin and cellulose model compounds during pyrolysis [15]. It was found that by varying the ratios between Lignin Pink and Cellulose Microcrystalline (Figure 1), the thermochemical process outcome is altered. This is where increased lignin content alters the reaction selectivity to generate more char. However, when compared to a ‘real’ feedstock, such as olive kernels or corn cobs, the product mixtures are not the same. This is due to the feedstock variability, as mentioned previously, which operates a wide range of thermochemical and tar thermal cracking reactions that promote a different process due to an ‘additive rule’. As a continuation of this work, the model compounds underwent gasification across various temperatures and air ratio (λ) values, where air ratio represents the ratio of the gasification air content to the total stoichiometric air required for complete oxidation of a specific fuel. In line with our previously published work [15], an assumption was made that various agro-residues of interest could be fairly resembled with synthetic mixtures, composed only from cellulose and lignin. This is due to the relatively low hemicellulose content that exists in both woody and herbaceous lignocellulosic waste. It was assumed that the hemicellulose component would contribute a minor role during gasification due to its similarities to cellulose [16].

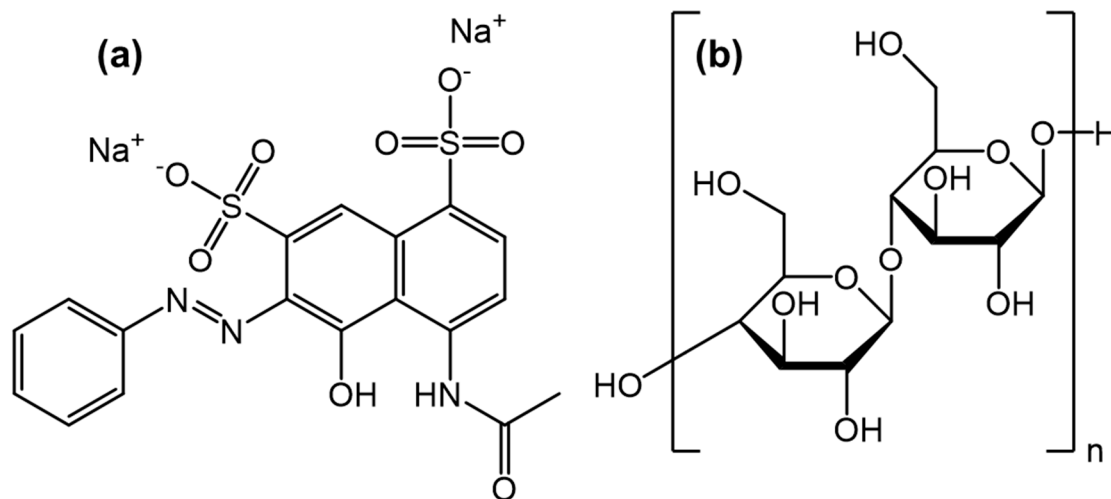


Figure 1. Model lignocellulosic biomass waste probe molecules: (a) Lignin Pink and (b) Cellulose Microcrystalline, derived from an α -cellulose precursor.

This work demonstrates the effect of lignin and cellulose model compound wt% ratios on the ratios of fuel gas species generated under varying gasification conditions, as well as the liquid and solid products. The selected gasification conditions are the ones most commonly used in autothermal industrial-scale woody biomass waste gasifiers [17]. Previously, for the pyrolysis of model compound mixtures, it was found that the char yield was enhanced for lignin-rich mixtures across all temperatures. An inverse trend was shown for tar where cellulose-rich mixtures were found to produce a higher tar selectivity [15]. Figure 1, as well as the ultimate analysis shown in our previous work [15], show that the lignin model compound Lignin Pink (LP) contains both Na and S, at 8.7 wt% and 12.6 wt%, respectively.

However, this contributes less than <0.1 wt% in ash content for the lignin model compound [15]. The ash values observed for pure lignocellulosic biomass feedstocks are much higher, ranging in some cases to >5 wt% [3]. Alternative waste feedstocks with higher inorganic contents are black liquor and pyrolysis oils as well as sludges produced during fossil-fired conventional energy generation [18]. It has previously been found that lignin thermochemical decomposition, specifically char degradation, can be promoted by Na [19]. This has also been shown for the LP compound [20]. High Na content in a model compound is comparable to real-world feedstocks such as olive cake [21], olive wood [22], poplar bark [22] and fir mill residues [22]. Na also exists in high concentrations in wheat straw [23] and buffalo gourd grass [22]. This behavior means that the presence of Na will force charring reactions, leading to an increase in gaseous products [20]. As the temperature of gasification increases from 800 °C, the rate of Na released into the gas phase increases in a non-linear fashion. This is because Na released to the gas phase at lower temperatures is transferred to the produced char-forming channels in the carbon interface during gasification [24], often forming larger mesopores than other alkali metals. This makes sodium, much like potassium and calcium, an edge-recession catalyst [24,25]. It has been shown that the presence of Na can effectively catalyze the water–gas shift reaction ($\text{CO} + \text{H}_2\text{O} \rightarrow \text{CO}_2 + \text{H}_2$), a mildly exothermic reaction, boosting the production of CO_2 and H_2 [24]. Although seen as less active than K for gasification, the Na present from the LP should provide a promotional effect on the gasification. The presence of residual ash is appropriate for this model reaction as pretreatments for most lignocellulosic waste feedstocks are not suitable for extracting all inorganics [3,11,12,26].

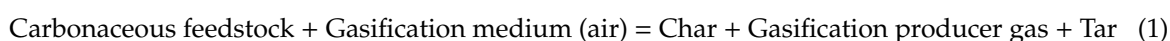
2. Materials and Methods

2.1. Sample Preparation and Characterization

Cellulose Microcrystalline (CM) and Lignin Pink (LP) were supplied by Sigma-Aldrich GmbH and Alfa Aesar U.S.A., respectively. Following the same method mentioned previously [15], the LP and CM model compounds were thoroughly mixed in weight percentages of 17 wt% LP, 83 wt% CM ($\text{LP}_{17}\text{CM}_{83}$) to generate a lignin-deficient material and 48 wt% LP, 52 wt% CM ($\text{LP}_{48}\text{CM}_{52}$) to resemble a material with a higher lignin content to mirror the composition of herbaceous and woody ‘real’ feedstocks such as alfalfa, pine straw and flax fiber [27]. Individual proximate and ultimate analyses of the model compounds are presented in earlier work, where data were obtained from the supplier directly [15].

2.2. Gasification Experimental Study

Similar to the experimental setup previously described in more detail [15], the gasification of CM and LP (particle sizes $d_p = 100\text{--}200 \mu\text{m}$) was carried out in a lab scale, downdraft fixed-bed stainless steel batch atmospheric reactor under a controlled reactive atmosphere. Here, synthetic air (O_2 20% and N_2 80%) was diluted by a mass flow controller with nitrogen to achieve the most commonly practiced gasification air ratios (λ) of 0.2, 0.3 and 0.4, at a flow rate of 20 mL/min, corresponding to ~0.4 s of gas residence time. The gasifier was heated to 750 and 850 °C, measured by a K-type thermocouple positioned in the sample holder of the reactor. The heating rate was calculated to be approximately 150 °C/min for a total reaction time of 20 min. Producer gas cleaning and subsequent sampling were carried out downstream from the reactor. Upon full gasification of the model compounds, the reactor was cooled and disassembled to reclaim the char residue. The total tar yield including the aqueous phase was determined by subtraction of the produced gaseous and char products, as illustrated by the overall general mass balance in Equation (1).



The most common gas phase products were sampled via airtight gas sampling bags and analyzed offline on an Agilent 6890N chromatograph fitted with two columns, HP-PlotQ and HP-Molsieve, with

FID and TCD detectors. More details on the specific experimental systems can be found in previous published works by the authors [12,15,28].

3. Product Analysis and Discussion

Figure 2a–d shows the product mix generated from the gasification with air of each of the model compound mixtures at two different temperatures (750 and 850 °C) and three different reaction atmospheres ($\lambda = 0.2, 0.3, 0.4$), corresponding to different under-stoichiometric air ratios and starting from the pure lignin (LP₁₀₀) in Figure 2a and decreasing to a rich-in-lignin mixture, diluted with cellulose LP₄₈CM₅₂ (Figure 2b), a low-lignin mixture LP₁₇CM₈₃ (Figure 2c) and the pure cellulose CM₁₀₀ (Figure 2d). In our previous pyrolysis study, we found that the char yields were enhanced when using lignin-rich mixtures [15]. However, in all cases (temperature and air ratio) for gasification this trend was not seen. In fact, the LP alone facilitated a far greater tar yield (Figure 2a) where it was found that ~25–30 wt% of the product mix was tar based on $\lambda = 0.2$ and 0.3 conditions, corresponding to the high-temperature pyrolytic stage of gasification. This might be attributed to the role of Na cations liberated during the thermal decomposition of the LP. Not only is the lignin decomposition pathway enhanced by Na, but dehydration, demethoxylation (-OCH₃) and decarboxylation (-COOH) reactions as well as char formation have previously been found to be catalyzed [29]. Although found to enhance various reactions, Na has been found to decrease the yield of organic volatiles and CO [29]. This has been echoed by Huang et al. who show that the reactivity of lignocellulosic chars increases with the addition/presence of metals. The order of promotion decreases down the following series, K > Na > Ca > Fe > Mg [30]. The major products intended from gasification are fuel gases. Figure 2b shows that by using the lignin-rich LP₄₈CM₅₂ mixture at 850 °C there is a substantial selectivity change from char to gas. Over 64 wt% of the product mix was gas for an air ratio of $\lambda = 0.4$, whereas for the same mixture at 750 °C under the same λ value there was only 25 wt% gas produced overall. It is clear from Figure 2a that overall, LP is responsible for low gas yields, as compared with mixtures and pure CM, Figure 2d, at 750 °C. By considering the gasification of the pure cellulose (CM₁₀₀) (Figure 2d), there was a maximum of 22.7 wt% gas produced, although for the CM a maximum char yield of 74 wt% could be obtained by using $\lambda = 0.3$ at 750 °C. With the exception of the pure lignin sample (LP₁₀₀), a maximum tar yield was generated for all mixtures in the lowest air ratio conditions ($\lambda = 0.2$), as was expected. It is clear that gasification under conditions of higher λ ratios in the reactor promotes char decomposition rather than restricting formation, especially at 850 °C (Figure 2b,c).

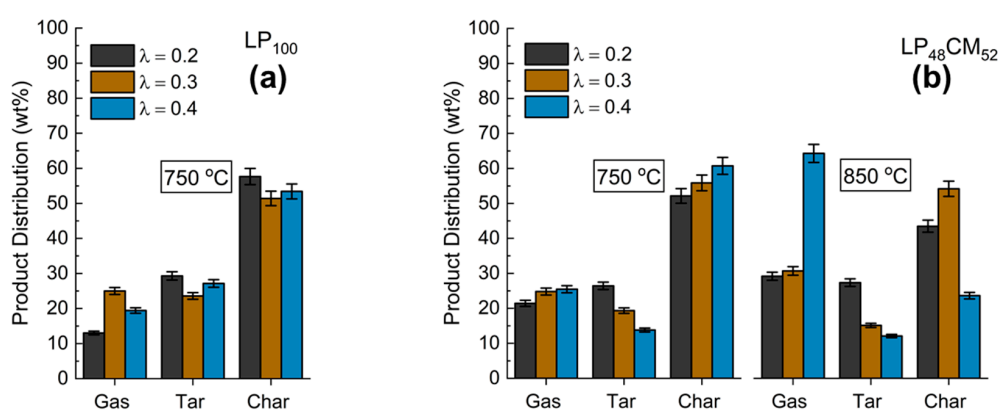


Figure 2. Cont.

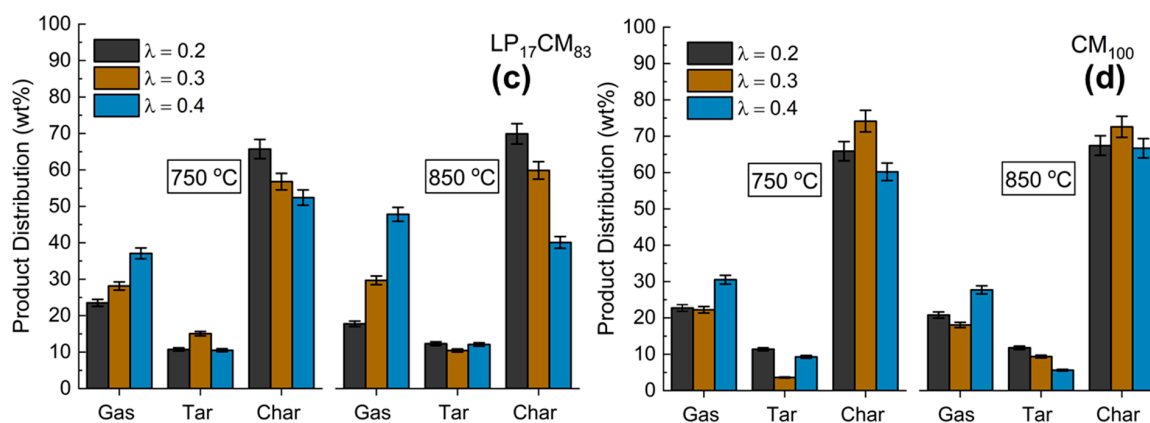


Figure 2. Product distribution of: (a) LP₁₀₀, (b) LP₄₈CM₅₂, (c) LP₁₇CM₈₃ and (d) CM₁₀₀ at two different gasification temperature parameters, 750 and 850 °C. Air content in the flux is indicated by λ .

To determine the effect of reactant synergies, the gas product (normalized, excluding N₂) selectivities are presented in Figure 3a,d, where Figure 3a is the undiluted LP₁₀₀ at 750 °C, while Figure 3b is LP₄₈CM₅₂, Figure 3c is LP₁₇CM₈₃ and Figure 3d is the undiluted CM₁₀₀ sample, at both operational temperatures. For the low-temperature gasification (750 °C) of LP under $\lambda = 0.2$, far more H₂ and CO are formed as compared with the higher air ratio ($\lambda = 0.4$). This is where a decrease of 41% and 30% was observed for H₂ and CO, respectively. As the O₂ concentration was increased in the stream, the fuel gas selectivity dropped significantly, favored by the richer oxygen atmosphere and residual Na in the form of Na₂CO₃ decomposing to form CO₂. By diluting the lignin content within the mixture, Figure 3b shows that the production of both CO and H₂ has increased dramatically at 850 °C. These data also show that by increasing the air content, there is an increase in the selectivity of CO opposed to CO₂, as shown in Figure 3a. Mixing the two compounds together results in a profound decrease in CH₄ production (Figure 3b,c) at both temperatures, as compared with LP₁₀₀ (750 °C, $\lambda = 0.2$) and CM₁₀₀ (850 °C, $\lambda = 0.2$). For the low temperature gasification of LP₁₇CM₈₃ (Figure 3c), there is a large switch in selectivity towards CO₂ across all λ values. At its maximum ($\lambda = 0.3$), 52% of the product mix was CO₂. For the same reaction conditions, this was 14.3% and 26.1% higher for LP₁₀₀ and LP₄₈CM₅₂, respectively. However, the lower lignin-containing mixture (Figure 3c) produces far less CO than LP₄₈CM₅₂, as shown in Figure 3b. This mixture shows a true synergistic effect between both compounds as the H₂ and CO production is far higher than LP₁₀₀ (Figure 3a) or CM₁₀₀ (Figure 3d) alone. Figure 3d reports the highest selectivities towards ethylene (C₂H₄) and ethane (C₂H₆), 0.8% and 1.0%, when operating at 850 °C and $\lambda = 0.2$. As the oxygen is increased in the stream, the selectivity of these two molecules drops to 0.5% and 0.1%, respectively. Interestingly, this drop is only observed for LP₄₈CM₅₂ (Figure 3b) where there is no production of ethylene or ethane. CM₁₀₀, when gasifying at 750 °C and $\lambda = 0.4$, was found to possess more combustion characteristics, producing 50.4% of CO₂ (Figure 3d). Although higher than LP₁₀₀ under the same conditions, both mixed materials were found to produce less CO₂ across both temperatures, at $\lambda = 0.4$. Overall, from Figure 3 two general conclusions can be made: (a) the increase in gasification temperature leads to an increase in H₂ content in the producer gas. This is due to the water–gas shift reaction and the hydrogen-enriched gas mechanisms being temperature-dependent and commonly promoted at the industrial scale by alkali and alkaline-earth metal catalysts, such as Na [31]. Hydrogen is also liberated due to heavy volatiles cracking on the char matrix [15,28]. Additionally, (b) the effect of air ratio on the produced gasses is not directly connected with the reduction of H₂ concentration, and/or the increase in CO_x.

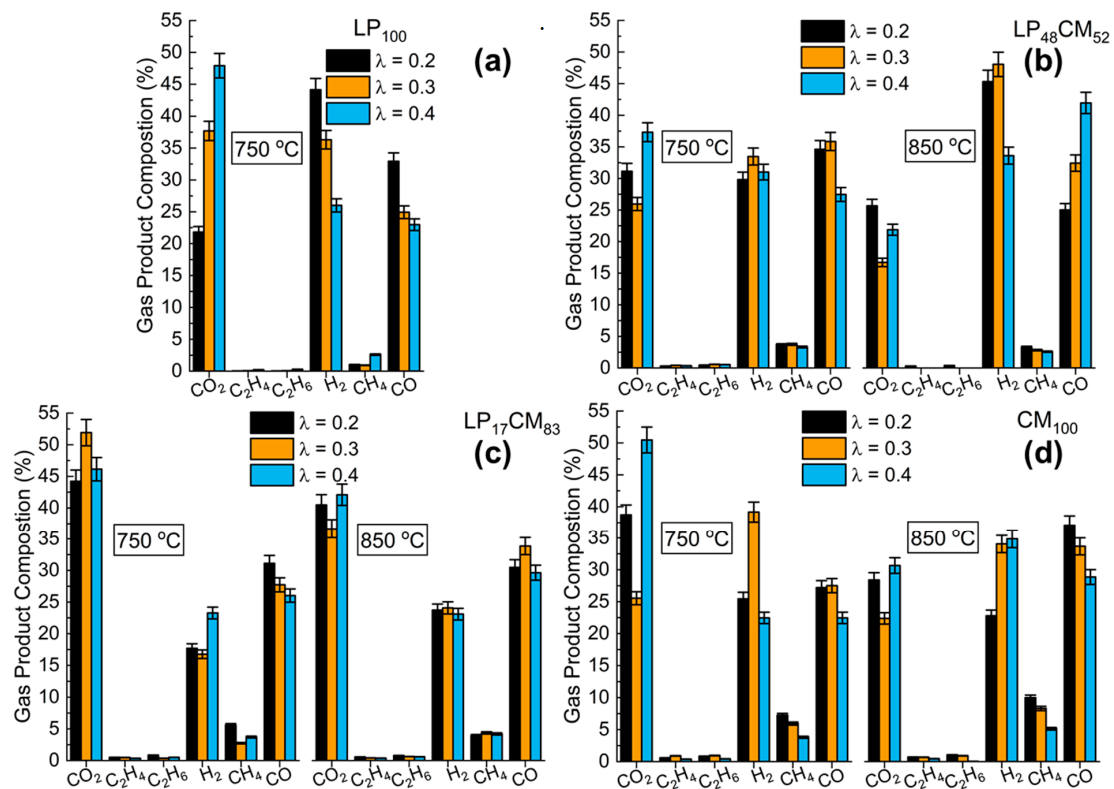


Figure 3. Gas phase product composition of: (a) LP₁₀₀, (b) LP₄₈CM₅₂, (c) LP₁₇CM₈₃ and (d) CM₁₀₀ at two different gasification temperature parameters, 750 and 850 °C. Air content in the flux is indicated by λ .

Figure 4a,b illustrates the correlation between the H₂ content and the CO_x in the producer gas at 750 and 850 °C, respectively. It is worth noting that in both figures a strong linear correlation between H₂ and CO/CO₂ is noticed. More specifically, the increase in carbon oxides (CO_x) in the producer gas decreases the production of H₂ and vice versa. Figure 4a shows that for LP₁₇CM₈₃ there is a greater concentration of CO_x molecules at 750 °C, across all air ratios (dark blue square). This is due to the greater char yields receiving a solid–gas reaction promotion from isolated Na deposits, donated by the LP. However, when operating at 850 °C there is not the same promotional effect observed for LP₁₇CM₈₃, but for the lignin-rich mixture (LP₄₈CM₅₂) there is a substantial decrease in char yield. It is suspected that the Na-rich deposits enhanced the water–gas shift reaction, thermochemically decomposing the char with reactively formed steam. Figure 4b shows that this effect is observed across all three reactions. This means that the O₂ content is not important as an equilibrium has been reached (red square). The greater Na effect is assumed to be attributed to the decomposition of char (Figure 2b). As char is decreased, the CO evolved readily reacts with produced steam in the reaction.

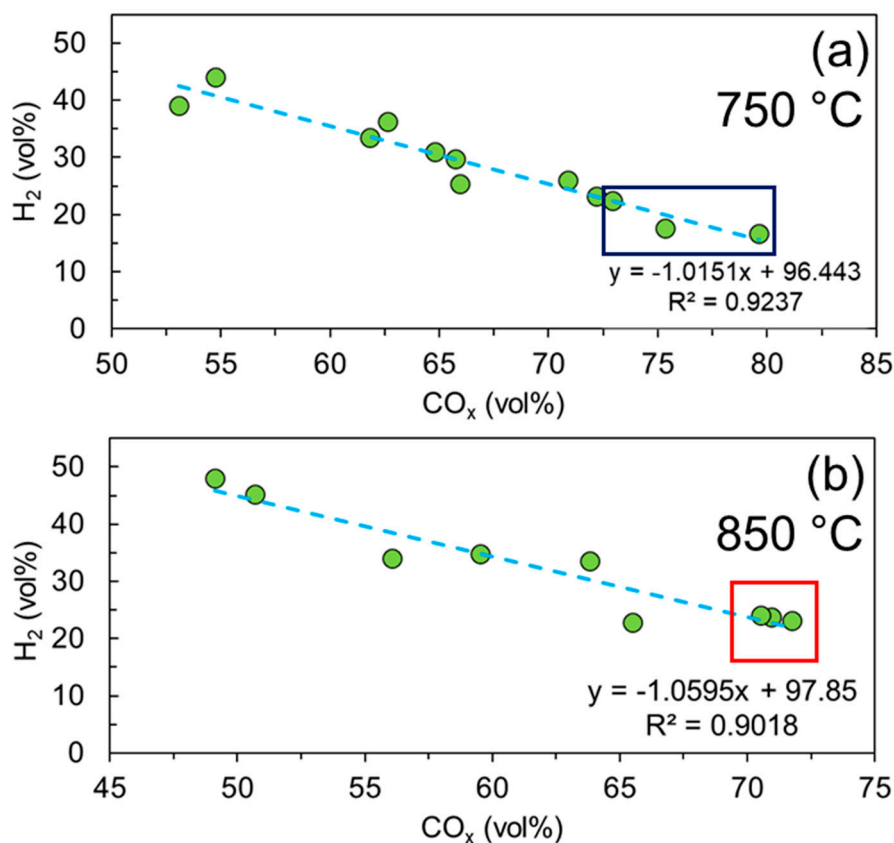


Figure 4. Correlation between hydrogen and carbon oxides at two different gasification temperatures: (a) 750 °C (dark blue square indicating LP₁₇CM₈₃) and (b) 850 °C (red square indicating LP₄₈CM₅₂), for all experimental mixtures and conditions.

4. Conclusions

The gasification of the model compound mixtures containing Lignin Pink and Cellulose Microcrystalline took place under the most common varying oxygen-containing atmospheres ($\lambda = 0.2, 0.3, 0.4$) and temperatures (750–850 °C) for current wood gasifiers. Here, varying ratios of the two compounds were used to examine the synergistic behavior between lignin and cellulose. An opposite trend was found to what was observed previously in our pyrolysis study: that char yields were enhanced when using lignin-rich mixtures. For gasification, it was found that cellulose-rich mixtures produced more char, while lignin-rich compounds produced a greater gas yield at 850 °C. We believe that this is due to the catalytic activity of Na in gasification, specifically at higher air content. As the Na forms channels decorating the surface of the formed char, gas phase reactions are promoted, specifically through the water–gas shift reaction, where reactively formed steam interacts with the char. It was found that the lignin-rich LP₄₈CM₅₂ mixture, when operating at 850 °C, provided the highest producer gas product mix. By increasing the Cellulose Microcrystalline content in the mixture, the oxidation process was accelerated where CO₂ was found to be the dominant product. In addition, a strong correlation between the produced H₂ and CO_x was observed. It was found that the Lignin Pink rich mixture received a substantial promotional effect from Na deposits decorating the surface of the char, enhancing the water–gas shift reaction and hydrogen enrichment mechanism when operating at 850 °C. As a result, the product mix was heavily pushed toward gas phase products as opposed to charring reactions at 750 °C. The significance of the presented results enhances the existing literature with a series of experimental results useful for simulation, modeling and validation studies for the pyrolysis and/or gasification of new-era wastes. Examples of such are feedstocks naturally

high in Na, sludges from NaOH delignification processes and alkaline metal ion-containing wastes from biorefineries.

Author Contributions: Conceptualization, V.S. and A.A.Z.; methodology, V.S.; software, M.J.T.; validation, M.J.T., A.K.M. and V.S.; formal analysis, M.J.T., A.K.M. and V.S.; investigation, V.S. and A.A.Z.; resources, A.A.Z.; data curation, V.S.; writing—original draft preparation, M.J.T.; writing—review and editing, M.J.T., A.K.M. and V.S.; visualization, A.K.M. and V.S.; supervision, V.S.; project administration, V.S.; funding acquisition, V.S. All authors have read and agreed to the published version of the manuscript.

Funding: V.S. acknowledges partial funding from (IKY 2010, Greece). V.S. and M.J.T. both acknowledge partial funding from the EPSRC (EP/P034667/1) and the THYME project (UKRI, Research England).

Acknowledgments: The authors would like to thank G. Stavropoulos (Aristotle University of Thessaloniki) for his support in providing both chemicals and the experimental rig.

Conflicts of Interest: The authors declare no conflict of interest.

References

1. Burnham, A.; Han, J.; Clark, C.E.; Wang, M.; Dunn, J.B.; Palou-Rivera, I. Life-cycle greenhouse gas emissions of shale gas, natural gas, coal, and petroleum. *Environ. Sci. Technol.* **2012**, *46*, 619–627. [[CrossRef](#)] [[PubMed](#)]
2. Haszeldine, R.S. Carbon capture and storage: How green can black be? *Science* **2009**, *325*, 1647–1652. [[CrossRef](#)]
3. Taylor, M.J.; Alabdrabalameer, H.A.; Skoulou, V. Choosing Physical, Physicochemical and Chemical Methods of Pre-Treating Lignocellulosic Wastes to Repurpose into Solid Fuels. *Sustainability* **2019**, *11*, 3604. [[CrossRef](#)]
4. Chen, H.Y.; Liu, J.B.; Chang, X.; Chen, D.M.; Xue, Y.; Liu, P.; Lin, H.L.; Han, S. A review on the pretreatment of lignocellulose for high-value chemicals. *Fuel Process. Technol.* **2017**, *160*, 196–206. [[CrossRef](#)]
5. Bahcivanji, L.; Gasco, G.; Paz-Ferreiro, J.; Mendez, A. The effect of post-pyrolysis treatment on waste biomass derived hydrochar. *Waste Manag.* **2020**, *106*, 55–61. [[CrossRef](#)]
6. Akubo, K.; Nahil, M.A.; Williams, P.T. Pyrolysis-catalytic steam reforming of agricultural biomass wastes and biomass components for production of hydrogen/syngas. *J. Energy Inst.* **2019**, *92*, 1987–1996. [[CrossRef](#)]
7. Wyn, H.K.; Zárate, S.; Carrascal, J.; Yermán, L. A Novel Approach to the Production of Biochar with Improved Fuel Characteristics from Biomass Waste. *Waste Biomass Valorization* **2019**. [[CrossRef](#)]
8. Wang, T.; Long, H.A. Techno-economic analysis of biomass/coal Co-gasification IGCC systems with supercritical steam bottom cycle and carbon capture. *Int. J. Energy Res.* **2014**, *38*, 1667–1692. [[CrossRef](#)]
9. Tarelho, L.A.C.; Neves, D.S.F.; Matos, M.A.A. Forest biomass waste combustion in a pilot-scale bubbling fluidised bed combustor. *Biomass Bioenergy* **2011**, *35*, 1511–1523. [[CrossRef](#)]
10. Liakakou, E.T.; Vreugdenhil, B.J.; Cerone, N.; Zimbardi, F.; Pinto, F.; André, R.; Marques, P.; Mata, R.; Girio, F. Gasification of lignin-rich residues for the production of biofuels via syngas fermentation: Comparison of gasification technologies. *Fuel* **2019**, *251*, 580–592. [[CrossRef](#)]
11. Taylor, M.J.; Alabdrabalameer, H.A.; Michopoulos, A.K.; Volpe, R.; Skoulou, V. Augmented Leaching Pretreatments for Forest Wood Waste and Their Effect on Ash Composition and the Lignocellulosic Network. *ACS Sustain. Chem. Eng.* **2020**, *8*, 5674–5682. [[CrossRef](#)]
12. Vaskalis, I.; Skoulou, V.; Stavropoulos, G.; Zabaniotou, A. Towards Circular Economy Solutions for The Management of Rice Processing Residues to Bioenergy via Gasification. *Sustainability* **2019**, *11*, 6433. [[CrossRef](#)]
13. de Lasa, H.; Salaices, E.; Mazumder, J.; Lucky, R. Catalytic steam gasification of biomass: Catalysts, thermodynamics and kinetics. *Chem. Rev.* **2011**, *111*, 5404–5433. [[CrossRef](#)] [[PubMed](#)]
14. Kuramochi, H.; Wu, W.; Kawamoto, K. Prediction of the behaviors of HS and HCl during gasification of selected residual biomass fuels by equilibrium calculation. *Fuel* **2005**, *84*, 377–387. [[CrossRef](#)]
15. Volpe, R.; Zabaniotou, A.A.; Skoulou, V. Synergistic Effects between Lignin and Cellulose during Pyrolysis of Agricultural Waste. *Energy Fuels* **2018**, *32*, 8420–8430. [[CrossRef](#)]
16. Basu, P. *Biomass Gasification, Pyrolysis and Torrefaction: Practical Design and Theory*, 2nd ed.; Elsevier Science: San Diego, CA, USA, 2013.
17. Mevissen, N.; Schulzke, T.; Unger, C.A.; Bhaird, S.M. Thermodynamics of autothermal wood gasification. *Environ. Prog. Sustain. Energy* **2009**, *28*, 347–354. [[CrossRef](#)]

18. Bach-Oller, A.; Furusjö, E.; Umeki, K. Fuel conversion characteristics of black liquor and pyrolysis oil mixtures: Efficient gasification with inherent catalyst. *Biomass Bioenergy* **2015**, *79*, 155–165. [[CrossRef](#)]
19. Fryda, L.A. Development of Advanced Power Production Systems with Biomass Utilization. Ph.D. Thesis, National Technical University of Athens, Athens, Greece, 2006.
20. Shen, D.; Hu, J.; Xiao, R.; Zhang, H.; Li, S.; Gu, S. Online evolved gas analysis by Thermogravimetric-Mass Spectroscopy for thermal decomposition of biomass and its components under different atmospheres: Part I. Lignin. *Bioresour. Technol.* **2013**, *130*, 449–456. [[CrossRef](#)]
21. Lapuerta, M.; Acosta, A.; Pazo, A. Fouling Deposits from Residual Biomass with High Sodium Content in Power Plants. *Energy Fuels* **2015**, *29*, 5007–5017. [[CrossRef](#)]
22. Vassilev, S.V.; Baxter, D.; Andersen, L.K.; Vassileva, C.G. An overview of the chemical composition of biomass. *Fuel* **2010**, *89*, 913–933. [[CrossRef](#)]
23. Xue, Z.; Zhong, Z.; Lai, X. Investigation on gaseous pollutants emissions during co-combustion of coal and wheat straw in a fluidized bed combustor. *Chemosphere* **2020**, *240*, 124853. [[CrossRef](#)] [[PubMed](#)]
24. Arnold, R.A.; Hill, J.M. Catalysts for gasification: A review. *Sustain. Energy Fuels* **2019**, *3*, 656–672. [[CrossRef](#)]
25. Baker, R.T.K.; Chludzinski, J.J. Catalytic Gasification of Graphite by Calcium and Nickel Calcium. *Carbon* **1985**, *23*, 635–644. [[CrossRef](#)]
26. Saidur, R.; Abdelaziz, E.A.; Demirbas, A.; Hossain, M.S.; Mekhilef, S. A review on biomass as a fuel for boilers. *Renew. Sustain. Energy Rev.* **2011**, *15*, 2262–2289. [[CrossRef](#)]
27. Watkins, D.; Nuruddin, M.; Hosur, M.; Tcherbi-Narteh, A.; Jeelani, S. Extraction and characterization of lignin from different biomass resources. *J. Mater. Res. Technol.* **2015**, *4*, 26–32. [[CrossRef](#)]
28. Skoulou, V.; Zabaniotou, A.; Stavropoulos, G.; Sakelaropoulos, G. Syngas production from olive tree cuttings and olive kernels in a downdraft fixed-bed gasifier. *Int. J. Hydrogen Energy* **2008**, *33*, 1185–1194. [[CrossRef](#)]
29. Jakab, E.; Faix, O.; Till, F.; Szekely, T. The Effect of Cations on the Thermal-Decomposition of Lignins. *J. Anal. Appl. Pyrolysis* **1993**, *25*, 185–194. [[CrossRef](#)]
30. Huang, Y.; Yin, X.; Wu, C.; Wang, C.; Xie, J.; Zhou, Z.; Ma, L.; Li, H. Effects of metal catalysts on CO₂ gasification reactivity of biomass char. *Biotechnol. Adv.* **2009**, *27*, 568–572. [[CrossRef](#)]
31. Ebadi, A.G.; Hisoriev, H.; Zarnegar, M.; Ahmadi, H. Hydrogen and syngas production by catalytic gasification of algal biomass (*Cladophora glomerata* L.) using alkali and alkaline-earth metals compounds. *Environ. Technol.* **2019**, *40*, 1178–1184. [[CrossRef](#)]



© 2020 by the authors. Licensee MDPI, Basel, Switzerland. This article is an open access article distributed under the terms and conditions of the Creative Commons Attribution (CC BY) license (<http://creativecommons.org/licenses/by/4.0/>).